International Journal of Mathematics Trends and Technology
ISSN: 2231 – 5373 /doi:10.14445/22315373/IJMTT-V67I6P501
Volume 67 Issue 6, 1-20, June, 2021

An Oscillatory Flow of Jeffrey Fluid through an Irregular Channel in the Presence of Magnetic Field

KW. Bunonyo [1] & B. Okardi [2]

[1]*Department of Mathematics and Statistics, Federal University Otuoke, Otuoke, Nigeria*
[2]*Department of Computer Science and Informatics, Federal University Otuoke, Nigeria*

Abstract *- Atherosclerosis is a form of cardiovascular illness characterized by an accumulation of insoluble substances, cellular debris and inflammation in the innermost layer of the arterial wall. Statin drugs have been the primary method for treating atherosclerotic lesions, but recent research suggests that lifestyle changes, in particular consuming a diet rich in antioxidants, may be equally effective at preventing and potentially reversing the process of atherogenesis. In this research, we formulated mathematical models to study the effect of the antioxidants on the legion regression of an atherosclerosis at the biological, and the geometry of the irregularity caused by an oxidation shown as the first equation. The second equation is the momentum equation, which is the fluid flow equation, the third equation is the energy equation and finally, the fourth equation is the mass diffusion of cholesterol equation. The aforementioned equations were scaled and reduced to a system of an ordinary differential equation. The biological model led to analytical solutions of the velocity, concentration and temperature profiles. Mathematica codes were developed to simulate the effect of the governing parameters on the flow profiles. Through the use of these equations, applied mathematicians can supply cardiologists with means for simulating and numerically analyzing various lesion regression scenarios.*

Keywords — *Atherosclerosis, Heat, Jeffrey Fluid, Palm Oil, Oscillatory, Magnetic Field*

I. INTRODUCTION

Atherosclerosis is the condition in which an artery wall thickens as a result of the buildup of fatty materials such as cholesterol [4, 20].This syndrome usually affects arterial blood vessels and occurs in response to chronic inflammatory processes [4]. Many factors have been incriminated in triggering the inflammatory process [5, 21]. One of these is the accumulation of macrophages and white blood cells promoted by low-density lipoproteins. Inadequate removal of fats and cholesterol from the macrophages results in the formation of fatty streaks which ultimately lead to fibrous plaques [6].In animal studies, highly oxidized and degraded substances caused adverse biological effects including growth retardation, diarrhea, cellular damage, and even death [7–11]. Studies have also shown that heating edible fats at high temperatures and feeding these to animals increase the development of atherosclerotic lesions [8, 12–14]. Several observations suggest that a diet rich in oxidized fat can lead to atherosclerosis [2] and ultimately cardiovascular disease [3]. The edible oils and fats constitute our daily diet and as such stands the risk of consuming oxidized fat. They provide a large portion of our energy needs, supply essential fatty acids, and act as carriers for fat-soluble vitamins. However, chemical changes can lead to the production of oxidized products [1]. Palm oil is one of the world's most widely consumed oils. Palm oil contains equal portions of saturated and unsaturated fatty acids [15]. Palm oil also has a significant level of natural antioxidants and has little tendency to form gums and off-flavors [16, 17]. The effects of heated palm oil on lipid parameters as well as its ability to produce atherosclerosis have yet to be determined. In light of this, our study focused on the consumption of this unsaturated oil (cholesterol), its mixed with blood and then flows through an irregular channel caused by an oxidation at the walls of the vessel. [22] Investigated an oscillatory flow of blood though a channel, though without considering treatment. However, in this paper, the formulated mathematical models were solved analytically using the method of undetermined coefficients for velocity, mass concentration of cholesterol and temperature profiles respectively.

II. MATHEMATICAL FORMULATION

The fluid is a heterogeneous mixture of cholesterol and blood; it is incompressible MHD, viscous and conducting fluid. The irregularity is as a result of the oxidation of the unsaturated fluid such as palm oil, which inhibits the normal flow of the blood to tissues and other organs of the body. The mixture of palm oil with the blood is considered to be a Jeffrey Fluid, and it is customary that the flow is unidirectional due to the intervention of the heart and the valves in preventing backflow flow, [19]. The increase in temperature through radiative heat source is considered to be important in reducing the oxidation level over time and improves the blood circulation. Since blood is an MHD fluid, it important to consider that there is an influence of magnetic field reacting with cholesterol. The schematic diagram showing the flow of Jeffrey fluid through an irregular channel, induced by magnetic field, (See Figure 3.1) is presented as:

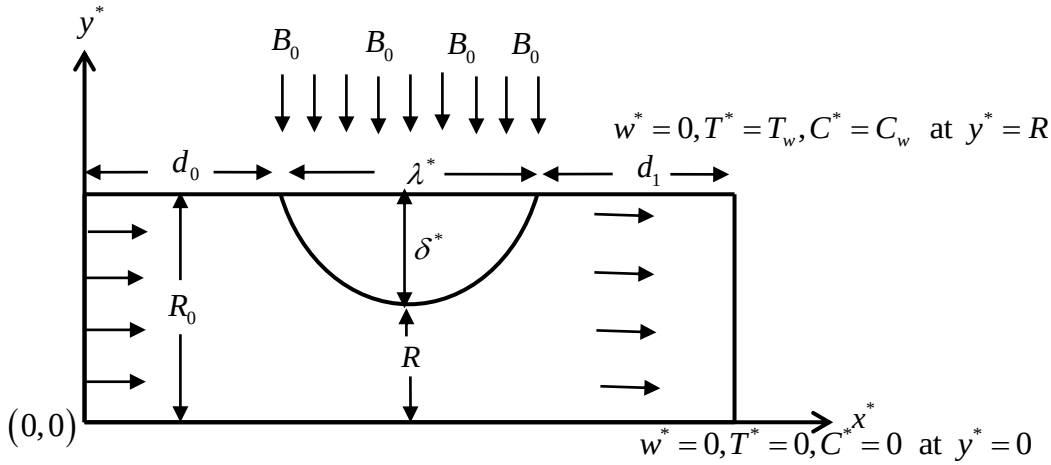

Figure 3.1: Schematic diagram showing the flow of Jeffrey fluid through an irregular channel, induced by magnetic field

We present the geometry of the irregular region as deduced from Figure 3.1, is:

$$R = \begin{cases} R_0 - \delta^* \left(cos 2\dfrac{\pi x^*}{\lambda^*} \right) & \text{at} \quad d_0 \le x^* \le \lambda^* \\ R_0 & \text{at} \quad 0 \le x^* \le d_0 \end{cases} \tag{3.1a}$$

where $x^* = \left(d_0 + \dfrac{\lambda}{2} \right)$

Following the consideration that the fluid flows through a channel and towards the axial direction and in view of the assumptions we present the following equations governing models

Continuity Equation

$$\frac{\partial w^*}{\partial x^*} = 0 \tag{3.1b}$$

Momentum Equation

$$\rho_b \frac{\partial w^*}{\partial t^*} = \begin{pmatrix} -\frac{\partial P^*}{\partial x^*} + \frac{\mu_b}{1+\lambda_1}\left(1+\lambda_2 \frac{\partial}{\partial t^*}\right)\frac{\partial^2 w^*}{\partial y^{*2}} - \sigma_e B_0^2 w^* - \frac{\mu_b \varphi}{k^*\left(1+\lambda_1\right)}\left(1+\lambda_2 \frac{\partial}{\partial t^*}\right)w^* \\ +\rho_b g \beta_T \left(T^* - T_\infty\right) + \rho_b g \beta_C \left(C^* - C_\infty\right) \end{pmatrix} \tag{3.2}$$

Energy Equation

$$\rho_b c_{bp} \frac{\partial T^*}{\partial t^*} = k_{bT} \frac{\partial^2 T^*}{\partial y^{*2}} + Q_0 \left(T^* - T_\infty\right) + Q_1 \left(C^* - C_\infty\right) \tag{3.3}$$

Mass Concentration Equation

$$\frac{\partial C^*}{\partial t^*} = D_m \frac{\partial^2 C^*}{\partial y^{*2}} - k_r \left(C^* - C_\infty\right) \tag{3.4}$$

The corresponding boundary conditions are as:

$$\left.\begin{aligned} w^* = 0, T^* = T_\infty, C^* = C_\infty \ \text{ at } \ y^* = 0 \\ w^* = 0, T^* = T_w, C^* = C_w \ \text{ at } \ y^* = R \end{aligned}\right\} \tag{3.5}$$

where Q_0 is the dimensional heat source of the fluid, k_b is the thermal conductivity of the fluid, Q_1 is the dimensional radiation absorption, T_∞ is far field temperature of the fluid, D_m is the molecular diffusivity of the fluid, ρ_b is the density of blood, σ_e is electrical conductivity, B_0 is the magnetic induction, k_r is the chemical reactant, c_b is the specific heat capacity of blood, β_T is the volumetric expansion, β_C is the volumetric expansion due to concentration, μ_b is the dynamic viscosity of blood, φ is the porosity, k^* is the permeability of the porous medium, λ_1 is the ratio of relaxation to retardation time, and λ_2 is the retardation time.

The following non-dimensional variables were introduced into equations (3.1a)-(3.6) to obtain the dimensionless equations.

$$\left.\begin{aligned} &\theta = \frac{T^* - T_\infty}{T_w - T_\infty}, \phi = \frac{C^* - C_\infty}{C_w - C_\infty}, Gr = \frac{g\beta_T \left(T_w - T_\infty\right) R_0^3}{\upsilon^2}, Gc = \frac{g\beta_C \left(C_w - C_\infty\right) R_0^3}{\upsilon^2}, \\ &Rd_2 = \frac{Q_1 \left(C^* - C_\infty\right) R_0^2}{k_T \left(T_w - T_\infty\right)}, Rd_3 = \frac{k_r R_0^2}{\upsilon} M = B_0 R_0 \sqrt{\frac{\sigma_e}{\mu_b}}, x = \frac{x^*}{\lambda}, y = \frac{y^*}{R_0}, w = \frac{w^* R_0}{\upsilon}, \\ &t = \frac{\upsilon t^*}{R_0^2}, \lambda = \frac{\lambda_2 \upsilon}{R_0^2}, \frac{1}{k} = \frac{\varphi R_0^2}{k^*}, Pr = \frac{\mu_b c_b}{k_T}, Rd_1 = \frac{Q_0 R_0^2}{\mu_b c_b} Sc = \frac{\upsilon}{D_m}, \end{aligned}\right\} \tag{3.7}$$

Following equation (3.7), we reduce equations (3.1b)-(3.6) dimensionless governing equations.

$$\frac{\partial w}{\partial t}=\left(\frac{1}{1+\lambda_1}\right)\left(1+\lambda\frac{\partial}{\partial t}\right)\frac{\partial^2 w}{\partial y^2}-M^2 w-\frac{1}{k}\left(\frac{1}{1+\lambda_1}\right)\left(1+\lambda\frac{\partial}{\partial t}\right)w+Gr\theta+Gc\phi \tag{3.8}$$

$$Pr\frac{\partial\theta}{\partial t}=\frac{\partial^2\theta}{\partial y^2}+\theta PrRd_1+\phi Rd_2 \tag{3.9}$$

$$\frac{\partial\phi}{\partial t}=\frac{1}{Sc}\frac{\partial^2\phi}{\partial y^2}-Rd_3\phi \tag{3.10}$$

The geometry of an atherosclerotic region is:

$$\frac{R}{R_0}=\begin{cases}1-\dfrac{\delta}{R_T}\left(cos2\pi x\right) & \text{at} \quad \dfrac{d_0}{\lambda}\le x\le 1\\ 1 & \text{at} \quad 0\le x\le\dfrac{d_0}{\lambda}\end{cases} \tag{3.11}$$

The corresponding boundary conditions are as:

$$\left.\begin{aligned} &w=0,\theta=0,\phi=0 && \text{at } y=0\\ &w=0,\theta=1,\phi=1 && \text{at } y=\frac{R}{R_0}=h\end{aligned}\right\} \tag{3.12}$$

III. METHOD OF SOLUTION

Since the flow is purely oscillatory, it is appropriate to seek for an oscillatory perturbation solution to in order to reduce the dimensionless coupled partial differential equation (3.8)-(3.12) to ordinary differential equations, [18].

$$\left.\begin{aligned} &w(y,t)=w_0(y)e^{i\omega t}\\ &\theta(y,t)=\theta_0(y)e^{i\omega t}\\ &\phi(y,t)=\phi_0(y)e^{i\omega t}\\ &\chi=\frac{y}{h}\end{aligned}\right\} \tag{3.13}$$

Substituting equation (3.13) into equations (3.8)-(3.12), we obtained the following ordinary differential equations:

$$\frac{\partial^2 w_0}{\partial y^2}-\left(\frac{M^2(1+\lambda_1)}{(1+\lambda i\omega)}+\frac{1}{k}+\frac{i\omega(1+\lambda_1)}{(1+\lambda i\omega)}\right)w_0+Gr\frac{(1+\lambda_1)}{(1+\lambda i\omega)}\theta_0+\frac{Gc(1+\lambda_1)}{(1+\lambda i\omega)}\phi_0=0 \tag{3.14}$$

$$\frac{\partial^2\theta_0}{\partial y^2}+(Rd_1-i\omega)Pr\theta_0=-\phi Rd_2 \tag{3.15}$$

$$\frac{\partial^2\phi_0}{\partial y^2}-(Rd_3+i\omega)Sc\phi_0=0 \tag{3.16}$$

Let $\beta_1 = h\left(\frac{M^2(1+\lambda_1)}{(1+\lambda i\omega)}+\frac{1}{k}+\frac{i\omega(1+\lambda_1)}{(1+\lambda i\omega)}\right), Gr_1 = Gr\,\frac{h(1+\lambda_1)}{(1+\lambda i\omega)}, Gc_1 = \frac{Gch(1+\lambda_1)}{(1+\lambda i\omega)}, \beta_2 = h(Rd_1 - i\omega)Pr$ and

$\beta_3 = h(Rd_3 + i\omega)Sc$, so that equation (3.14)-(3.16) are reduce to:

$$\frac{\partial^2 w_0}{\partial \chi^2} - \beta_1 w_0 = -Gr_1\theta_0 - Gc_1\phi_0 \tag{3.17}$$

$$\frac{\partial^2 \theta_0}{\partial \chi^2} + \beta_2\theta_0 = -\phi_0 hRd_2 \tag{3.18}$$

$$\frac{\partial^2 \phi_0}{\partial \chi^2} - \beta_3\phi_0 = 0 \tag{3.19}$$

The corresponding boundary conditions are as:

$$\left.\begin{aligned} &w_0 = 0, \theta_0 = 0, \quad \phi_0 = 0 \quad \text{at } \chi = 0 \\ &w_0 = 0, \theta_0 = e^{-i\omega t}, \phi_0 = e^{-i\omega t} \quad \text{at } \chi = 1 \end{aligned}\right\} \tag{3.20}$$

Solving for Mass concentration, we solve equation (3.19), and obtained the solution

$$\phi_0(\chi) = A_1 sinh\left(\sqrt{\beta_3}\chi\right) + B_1 cosh\left(\sqrt{\beta_3}\chi\right) \tag{3.21}$$

Solving for the constant coefficients in equation (3.21) using the corresponding boundary conditions in equation (3.20), we have:

$$\phi_0(\chi) = \left(\frac{e^{-i\omega t}}{sinh\left(\sqrt{\beta_3}\right)}\right) sinh\left(\sqrt{\beta_3}\chi\right) \tag{3.22}$$

To solve for the fluid temperature, substitute equation (3.22) into equation (3.18), we obtain the following:

$$\frac{\partial^2 \theta_0}{\partial \chi^2} + \beta_2\theta_0 = \beta_4 sinh\left(\sqrt{\beta_3}\chi\right) \tag{3.23}$$

where $\beta_4 = -\left(\frac{Rd_2 he^{-i\omega t}}{sinh\left(\sqrt{\beta_3}\right)}\right)$

The homogenous solution of equation (1.20) is

$$\theta_{0h}(\chi) = A_2 sin\left(\sqrt{\beta_2}\chi\right) + B_2 cos\left(\sqrt{\beta_2}\chi\right) \tag{3.24}$$

The particular solution of equation (3.23) is:

$$\theta_{0p}(\chi) = \left(\frac{\beta_4}{(\beta_2+\beta_3)}\right) sinh\left(\sqrt{\beta_3}\chi\right) \tag{3.25}$$

The solution of equation (3.23) is as follows:

$$\theta_0(\chi) = A_2 sin\left(\sqrt{\beta_2}\chi\right) + B_2 cos\left(\sqrt{\beta_2}\chi\right) + \left(\frac{\beta_4}{(\beta_2+\beta_3)}\right) sinh\left(\sqrt{\beta_3}\chi\right) \tag{3.26}$$

Solving for the constants coefficients of equation (3.26) using equation (3.20), we have the following:

$$\theta_0(\chi) = A_2 sin\left(\sqrt{\beta_2}\chi\right) + \left(\frac{\beta_4}{(\beta_2+\beta_3)}\right) sinh\left(\sqrt{\beta_3}\chi\right) \tag{3.27}$$

where $B_2 = 0, A_2 = \dfrac{e^{-i\omega t}}{sin\left(\sqrt{\beta_2}\right)} - \left(\dfrac{\beta_4}{(\beta_2+\beta_3)}\right)\dfrac{sinh\left(\sqrt{\beta_3}\right)}{sin\left(\sqrt{\beta_2}\right)}$

Substituting equation (3.27) and (3.22) into equation (3.17), we have the following:

$$\frac{\partial^2 w_0}{\partial \chi^2} - \beta_1 w_0 = -Gr_1 A_2 sinh\left(\sqrt{\beta_2}\chi\right) + \beta_5 sinh\left(\sqrt{\beta_3}\chi\right) \tag{3.28}$$

where $\beta_5 = \left(\left(\dfrac{\beta_4 Gr_1}{(\beta_2+\beta_3)}\right) + \left(\dfrac{Gc_1 e^{-i\omega t}}{sinh\left(\sqrt{\beta_3}\right)}\right)\right)$

The homogenous solution of equation (3.28) is:

$$w_{0h} = A_3 sinh\left(\sqrt{\beta_1}\chi\right) + B_3 cosh\left(\sqrt{\beta_1}\chi\right) \tag{3.29}$$

The particular solution of equation (1.25) is as follows:

$$w_{0p} = \left(\frac{Gr_1 A_2}{(\beta_2-\beta_1)}\right) sinh\left(\sqrt{\beta_2}\chi\right) + \left(\frac{\beta_5}{(\beta_1-\beta_3)}\right) sinh\left(\sqrt{\beta_3}\chi\right) \tag{3.30}$$

The solution of equation (3.17) is the sum of equation (3.29) and (3.30), it is as follows:

$$w_0 = A_3 sinh\left(\sqrt{\beta_1}\chi\right) + B_3 cosh\left(\sqrt{\beta_1}\chi\right) + \left(\frac{Gr_1 A_2}{(\beta_2-\beta_1)}\right) sin\left(\sqrt{\beta_2}\chi\right) + \left(\frac{\beta_5}{(\beta_1-\beta_3)}\right) sinh\left(\sqrt{\beta_3}\chi\right) \tag{3.31}$$

Solving for the constant coefficients of equation (3.31) using the boundary conditions in equation (3.20), it is as follows:

$$w_0 = A_3 sinh\left(\sqrt{\beta_1}\chi\right) + \left(\frac{Gr_1 A_2}{(\beta_2-\beta_1)}\right) sin\left(\sqrt{\beta_2}\chi\right) + \left(\frac{\beta_5}{(\beta_1-\beta_3)}\right) sinh\left(\sqrt{\beta_3}\chi\right) \tag{3.32}$$

where $A_3 = \left(\dfrac{Gr_1 A_2}{(\beta_1-\beta_2)}\right)\dfrac{sin\left(\sqrt{\beta_2}\right)}{sinh\left(\sqrt{\beta_1}\right)} + \left(\dfrac{\beta_5}{(\beta_3-\beta_1)}\right)\dfrac{sinh\left(\sqrt{\beta_3}\right)}{sinh\left(\sqrt{\beta_1}\right)}$

The velocity profile, temperature profile and concentration profile is obtained after substituting equation (3.32), (3.27) and (3.22) into equation (3.13) respectively as:

$$w(\chi)=\left(A_3 sinh\left(\sqrt{\beta_1}\chi\right)+\left(\frac{Gr_1 A_2}{(\beta_2-\beta_1)}\right)sin\left(\sqrt{\beta_2}\chi\right)+\left(\frac{\beta_5}{(\beta_1-\beta_3)}\right)sinh\left(\sqrt{\beta_3}\chi\right)\right)e^{i\omega t} \quad (3.31)$$

$$\theta(\chi)=\left(A_2 sin\left(\sqrt{\beta_2}\chi\right)+\left(\frac{\beta_4}{(\beta_2+\beta_3)}\right)sinh\left(\sqrt{\beta_3}\chi\right)\right)e^{i\omega t} \quad (3.32)$$

$$\phi(\chi)=\left(\left(\frac{e^{-i\omega t}}{sinh\left(\sqrt{\beta_3}\right)}\right)sinh\left(\sqrt{\beta_3}\chi\right)\right)e^{i\omega t} \quad (3.33)$$

IV. PRESENTATION OF SIMULATED RESULTS

In this section, we shall code the analytical solutions in equations (3.31)-(3.33) using a computation software called Mathematica, version 10.1. The simulation was carried out by varying each of the pertinent governing parameters such as the radiation parameter, Schmidt number, Grashof number, solutal Grashof number, height of stenosis, treatment parameter, periodic parameter, metabolic heat parameter, Hartmann number, and permeability parameter. The parameter values used in the simulation is within the range: and below are the results: some of the parameters values used in the simulation are:

$0 \le Ha \le 5, 0 \le Da \le 1, 0 \le \lambda_1 \le 5, 0 \le \lambda_2 \le 1,$

$Gr = 5,10,15,20,25, Gc = 5,10,15,20,25, Pr = 21, 0 \le Rd_1 \le 5, 0 \le Rd_2 \le 5, Rd_3 \le 5, 0 \le \delta \le 2$

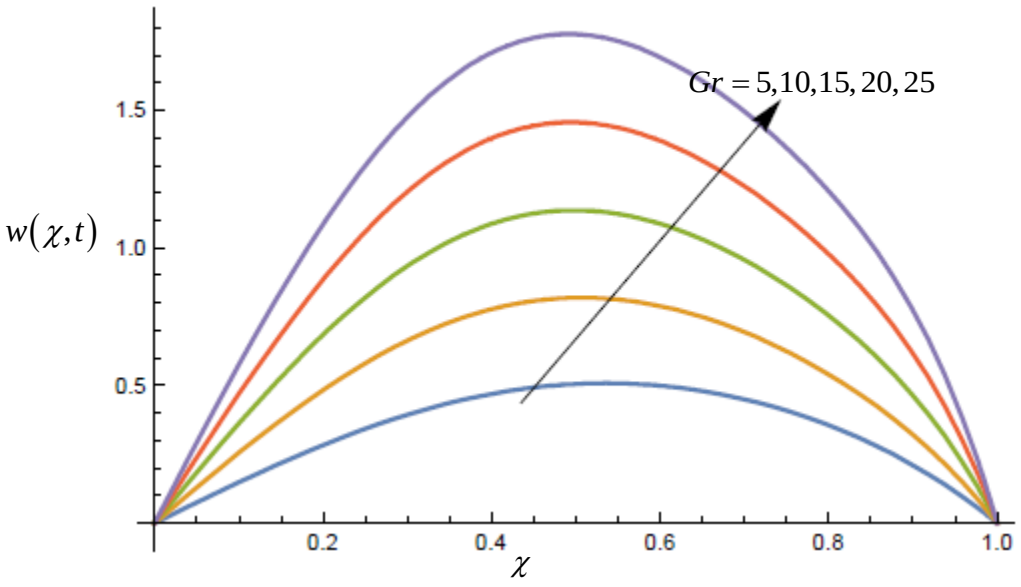

Figure 1.1: **Effect of Grashof parameter Gr values on velocity $w(\chi,t)$**

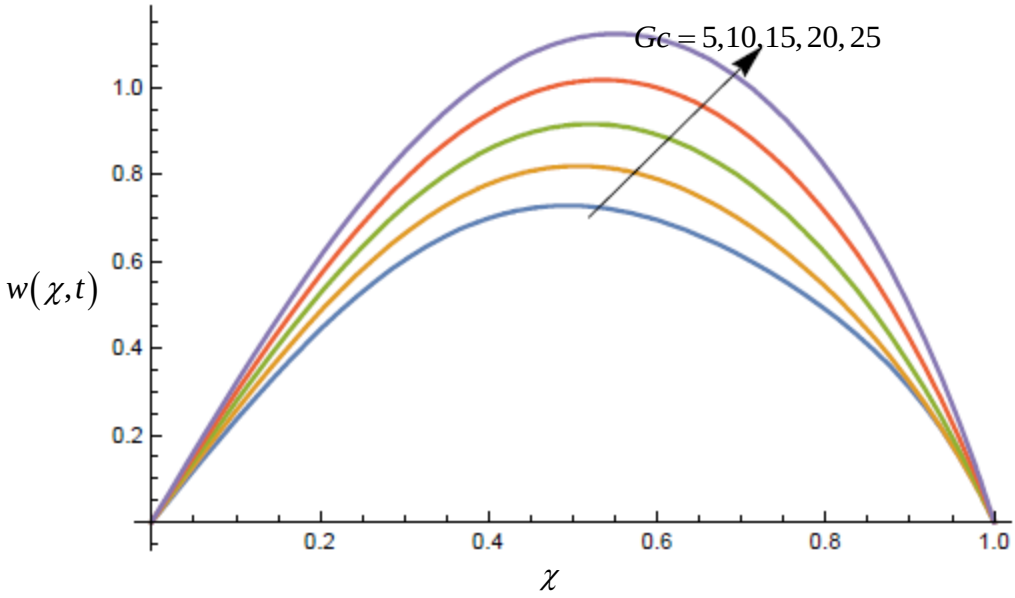

Figure 1.2: **Effect of solutal Grashof parameter** Gc **values on velocity** $w(\chi,t)$

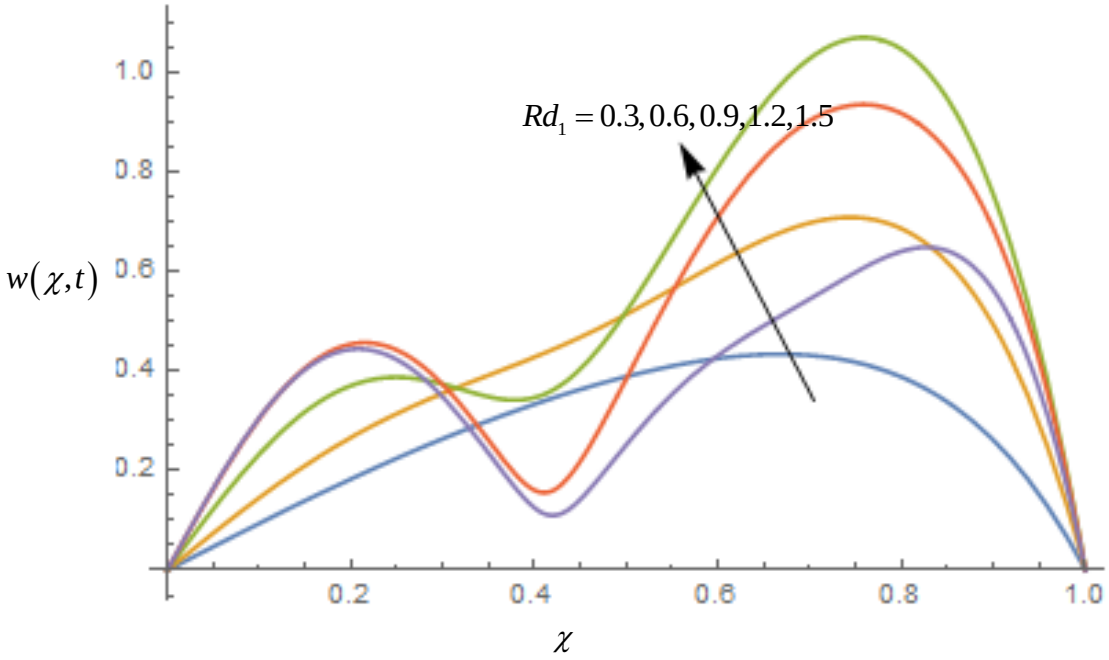

Figure 1.3: Effect of radiation parameter Rd_1 **values on velocity** $w(\chi,t)$

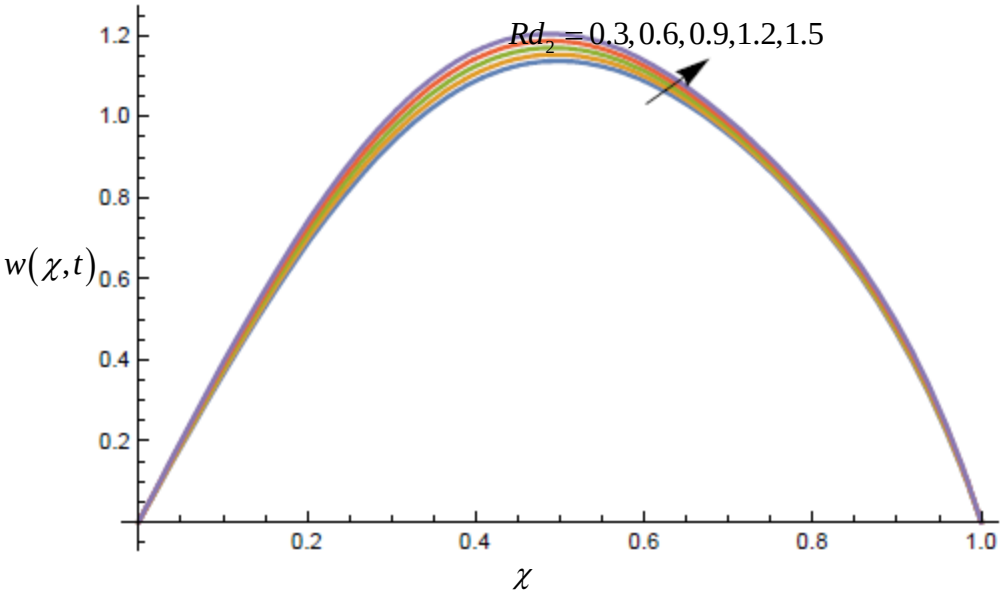

Figure 1.4: Effect of absorption parameter Rd_2 values on velocity $w(\chi,t)$

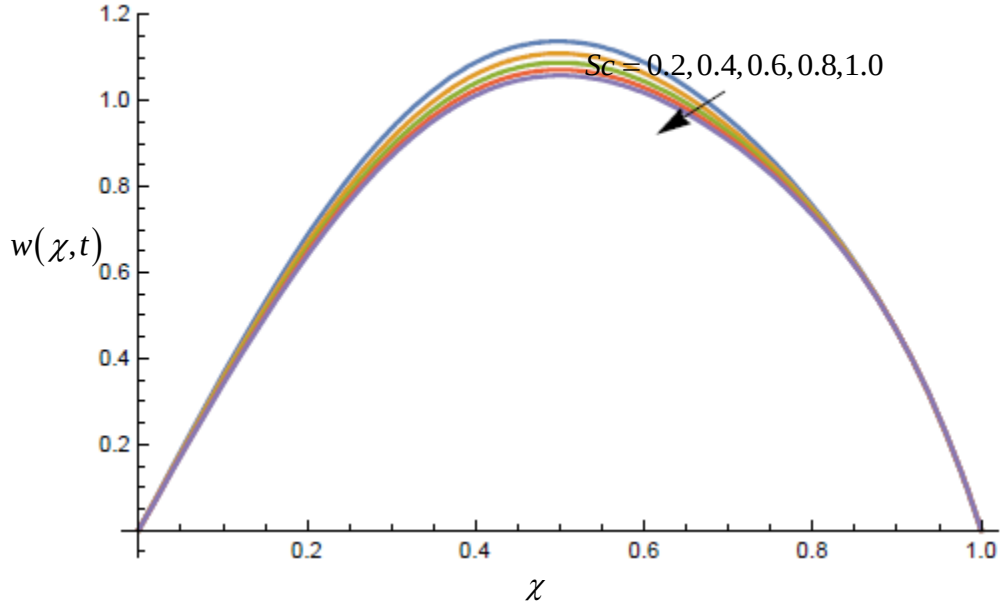

Figure 1.5: Effect of Schmidt number Sc values on velocity $w(\chi,t)$

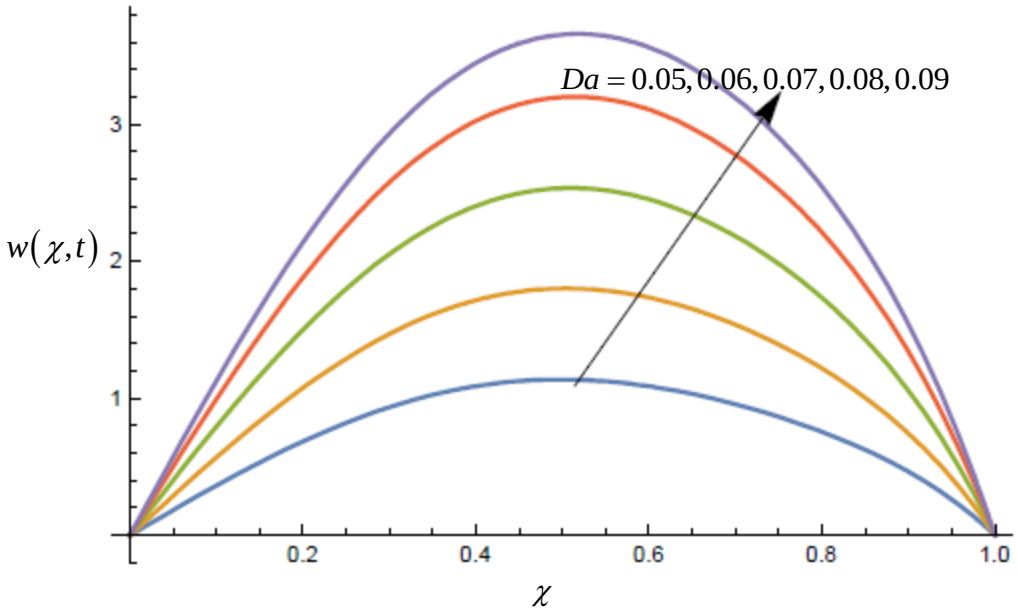

Figure 1.6: Effect of Darcy parameter Da values on velocity $w(\chi,t)$

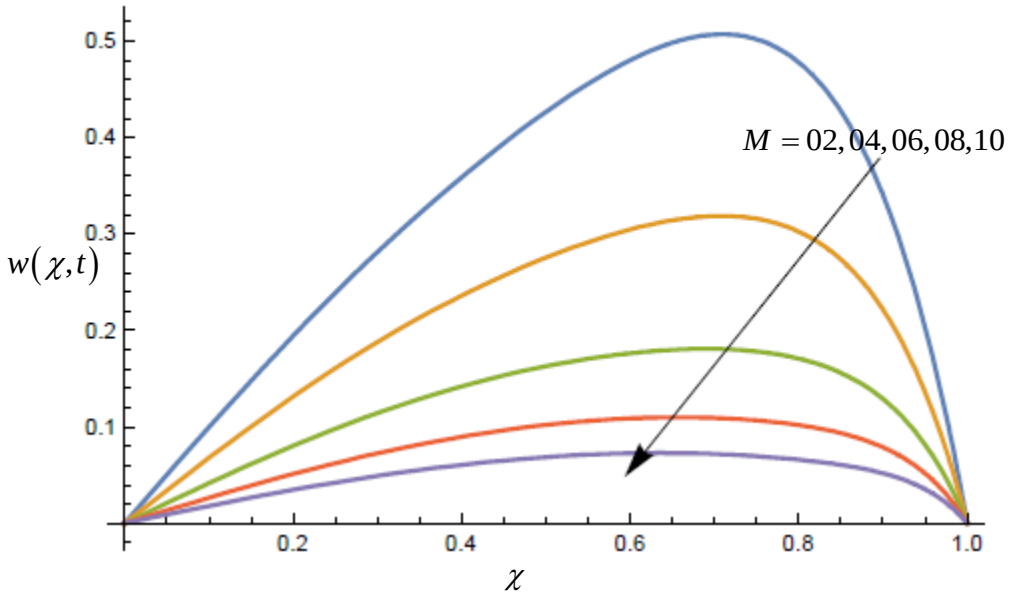

Figure 1.7: Effect of Hartmann number M values on velocity $w(\chi,t)$

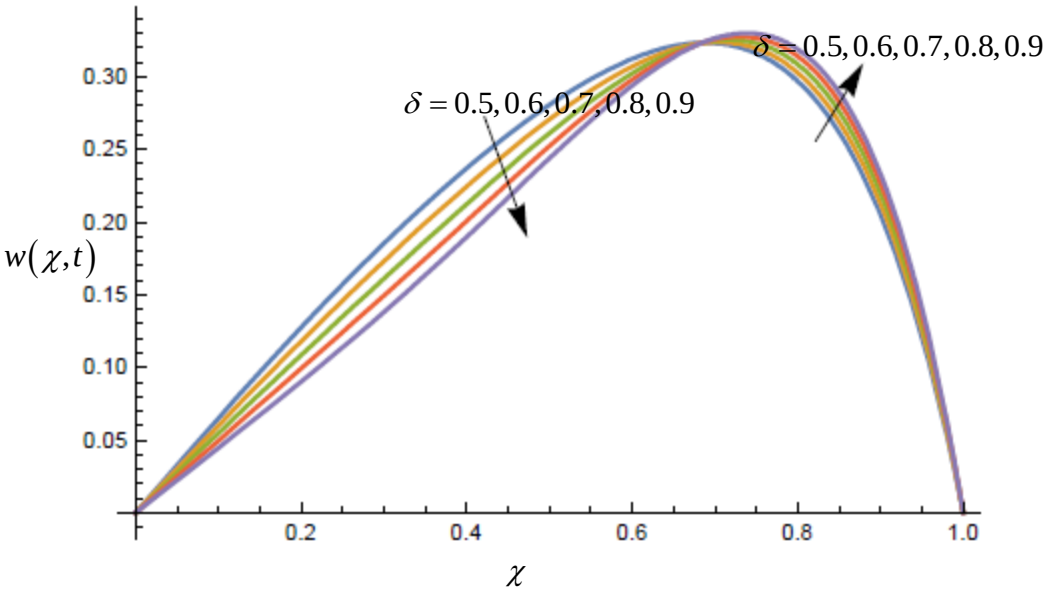

Figure 1.8: Effect of height of stenosis δ values on velocity $w(\chi, t)$

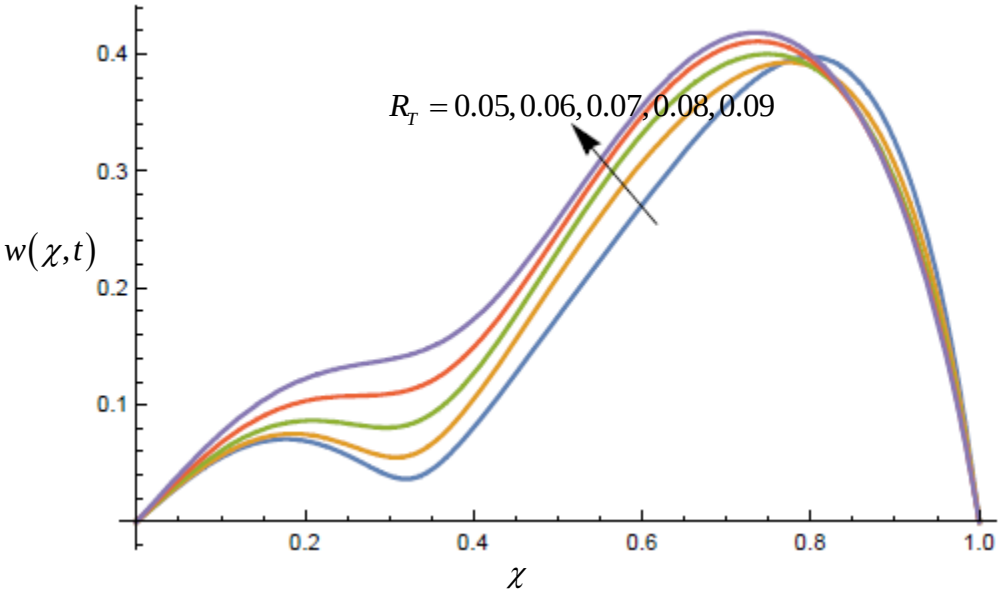

Figure 1.9: Effect of treatment parameter R_T values on velocity $w(\chi, t)$

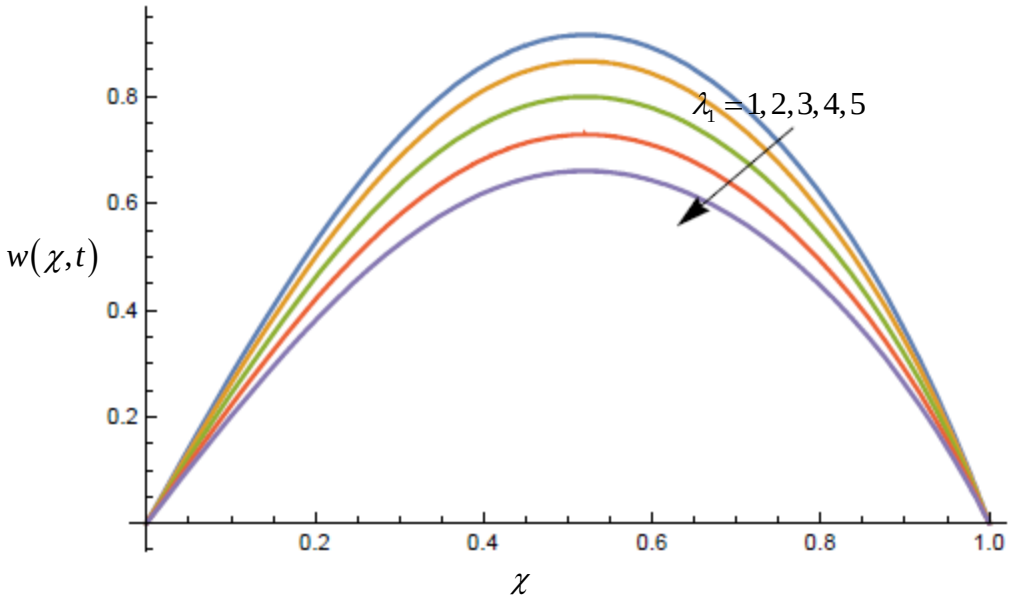

Figure 1.10: Effect of relaxation to retardation time parameter λ_1 values on velocity $w(\chi,t)$

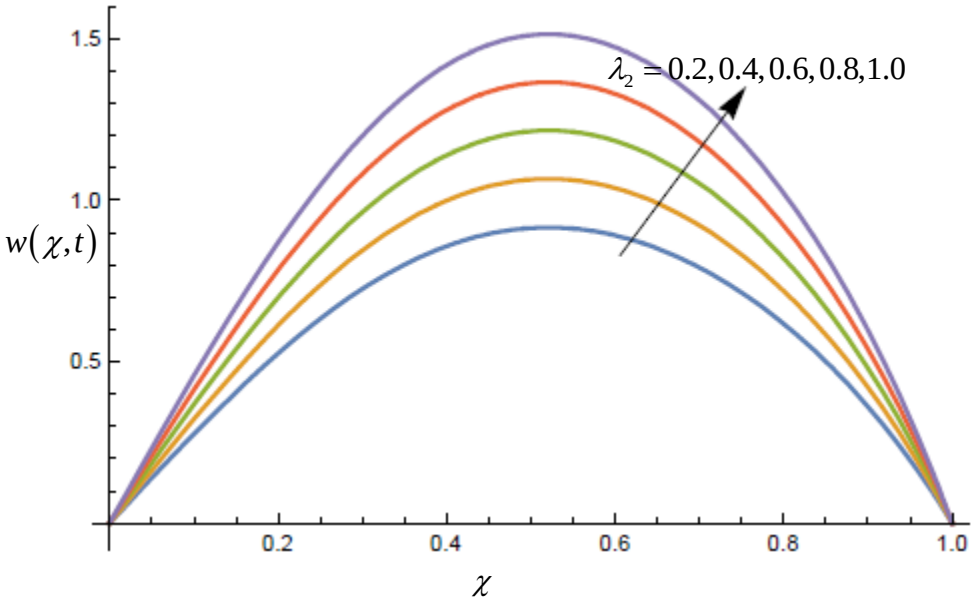

Figure 1.11: Effect of retardation time parameter λ_2 values on velocity $w(\chi,t)$

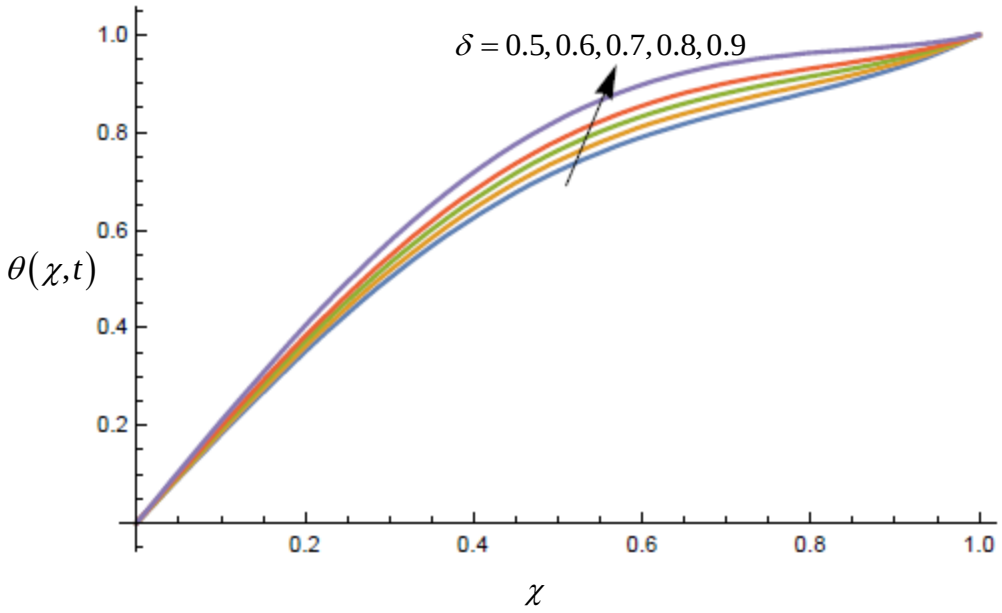

Figure 1.12: Effect of height of stenosis parameter δ values on temperature $\theta(\chi,t)$

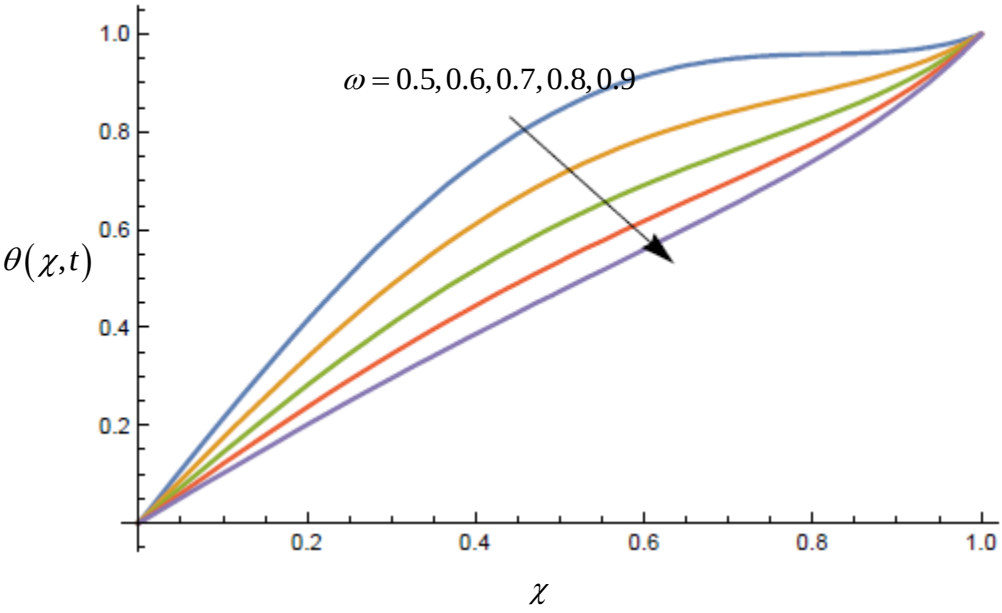

Figure 1.13: Effect of oscillatory frequency parameter ω values on temperature $\theta(\chi,t)$

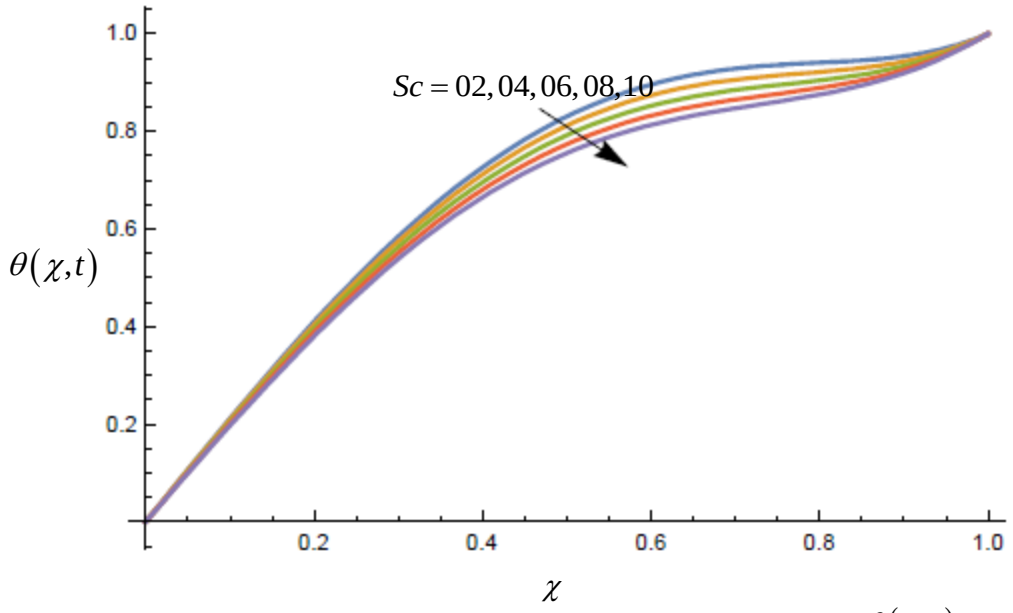

Figure 1.14: Effect of Schmidt number Sc values on temperature $\theta(\chi,t)$

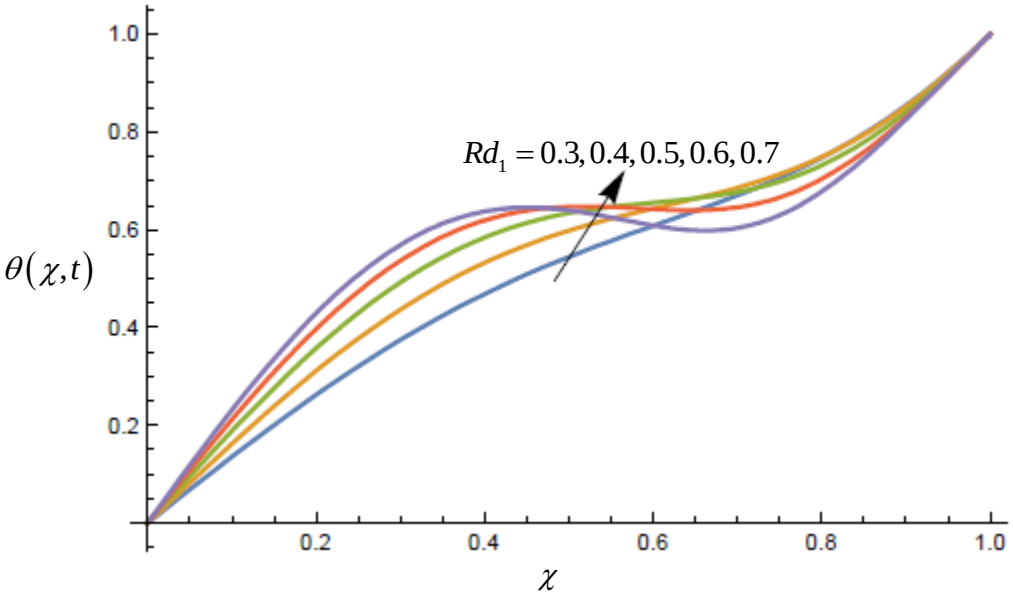

Figure 1.15: Effect of radiation parameter Rd_1 values on temperature $\theta(\chi,t)$

$$Rd_2 = 01, 02, 03, 04, 05$$

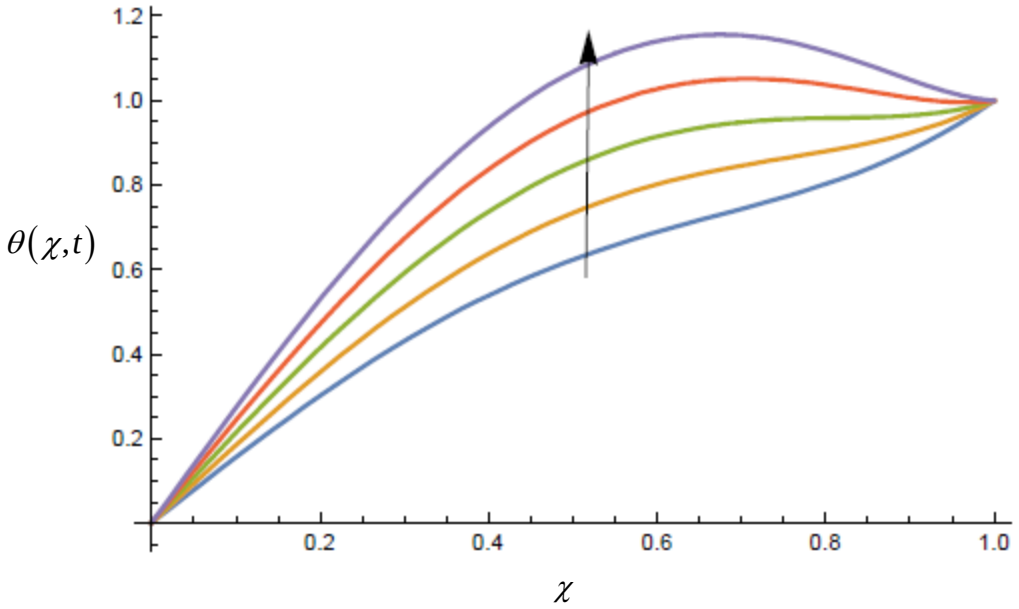

Figure 1.16: Effect of radiation absorption parameter Rd_2 values on temperature $\theta(\chi,t)$

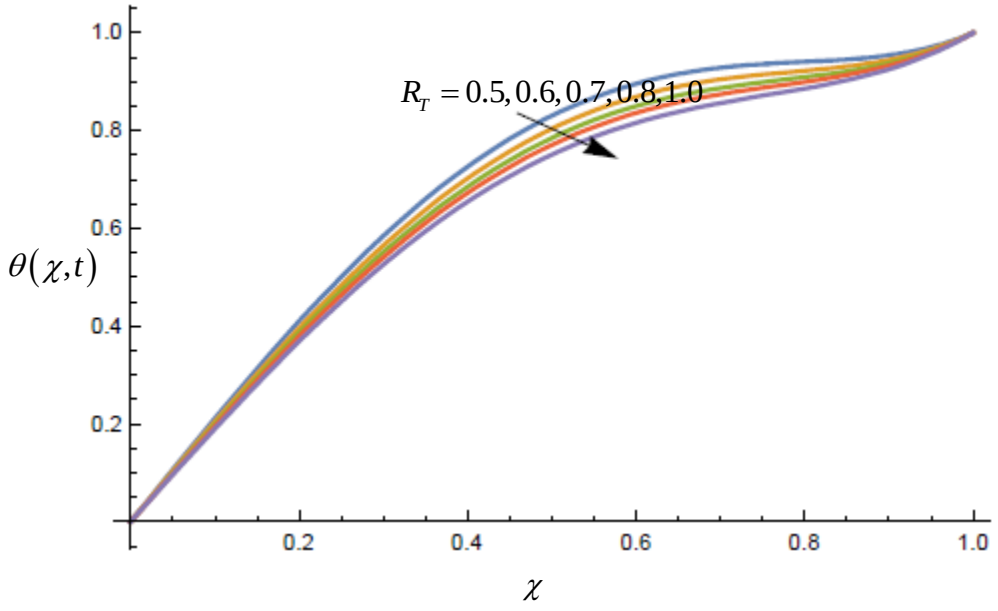

Figure 1.17: Effect of treatment parameter R_T values on temperature $\theta(\chi,t)$

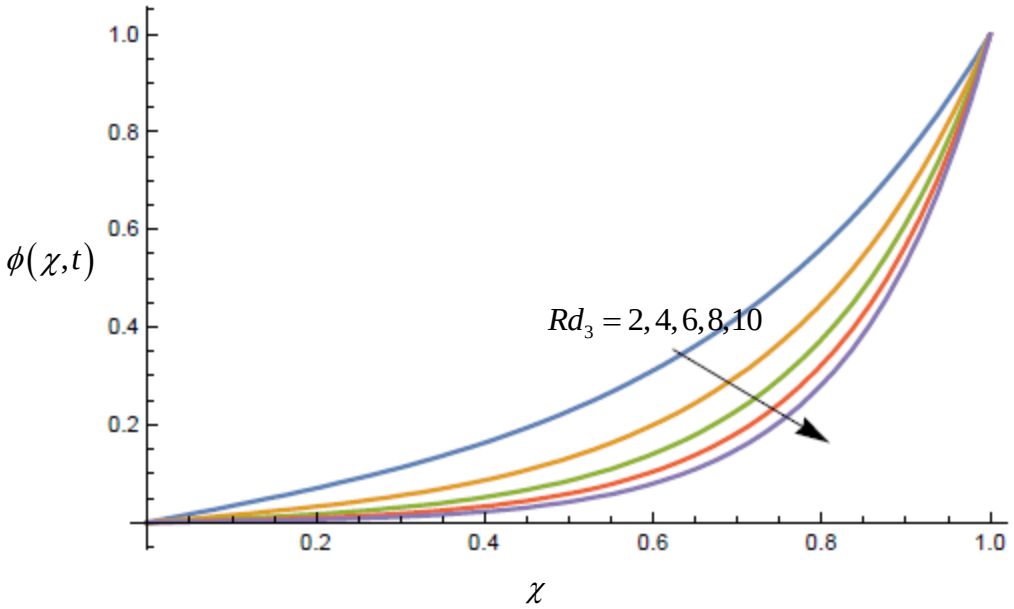

Figure 1.18: Effect of chemical reaction Rd_3 values on concentration $\phi(\chi,t)$

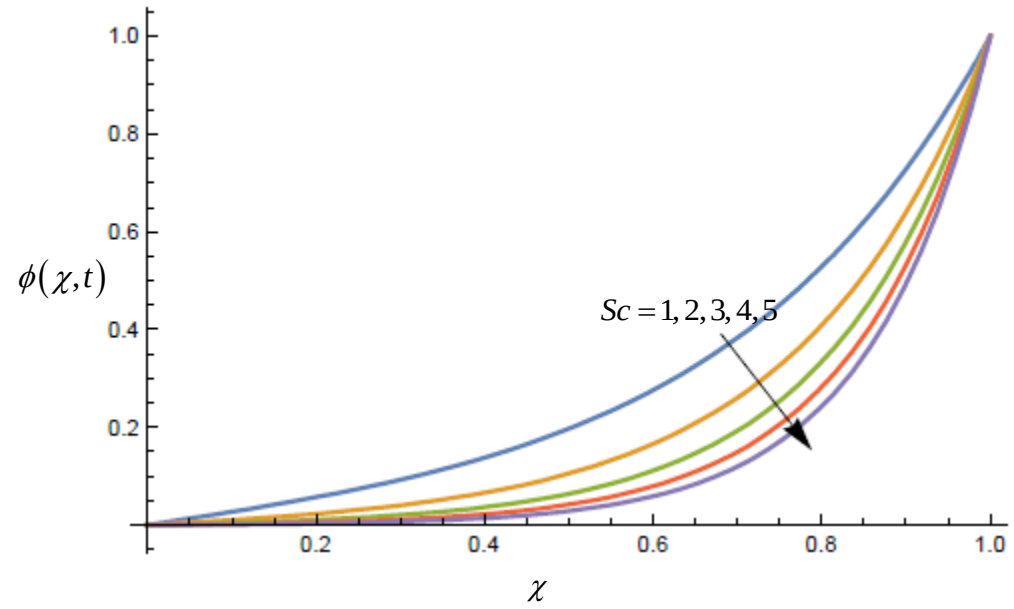

Figure 1.19: Effect of Schmidt number Sc values on concentration $\phi(\chi,t)$

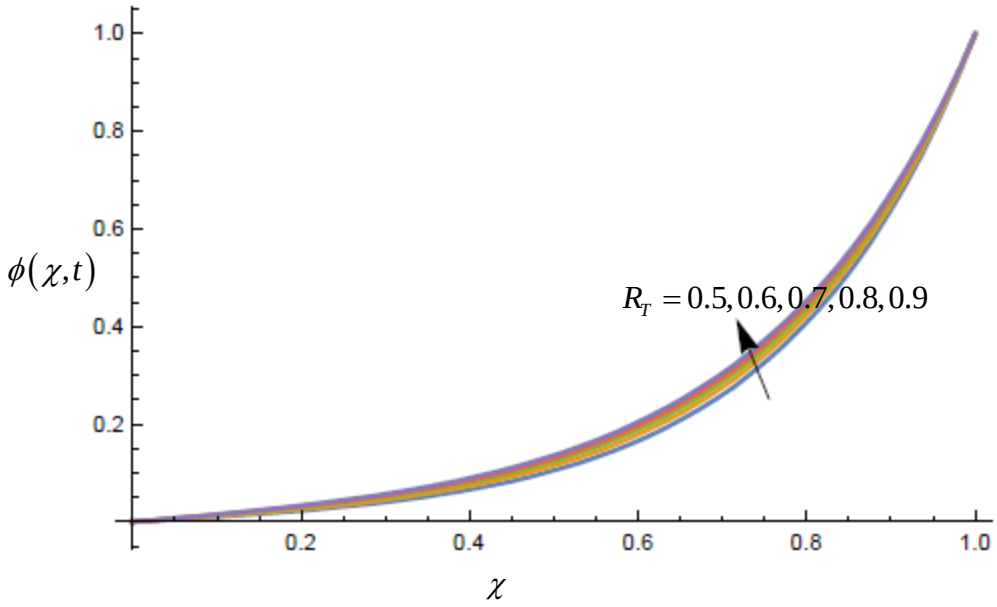

Figure 1.20: Effect of Treatment parameter R_T values on concentration $\phi(\chi,t)$

V. DISCUSSION AND CONCLUSION

The biological models led to an analytical solution of the velocity, mass cholesterol concentration and temperature profiles the flow profiles and the investigation revealed the following:

i. An increase in Grashof number Gr and solutal Grashof number Gc caused the velocity of the fluid to increase. This result is of the view that the velocity of the fluid increase as the buoyancy effect due to temperature and concentration is increased as seen in **Figure 1-2**.

ii. The Radiation of through heat source denoted with Rd_1 was investigated in this study and result denoted in **Figure 3**, and it was found that an increase in radiation caused a corresponding increase in the fluid velocity. This is of the view that the radiation increases cause an increase in the temperature of the fluid and as such reduces particles settling in one place.

iii. The chemical reaction between palm oil and blood with the other viscous constituents caused an increase in velocity. it is seen in **Figure 4** that the velocity increases for the increases in chemical reaction occasioned by the presence of other nutrients.

iv. **Figure 5** depicts that the velocity of the fluid decreases, for an increase in the Schmidt number. This clearly showed that the kinematics viscosity is greater that the molecular diffusion and this led to the decrease in velocity.

v. The Darcy number Da increase was investigated and results shown in **Figure 6**, the result depicts an increase in fluid velocity as the pores of the medium are increased.

vi. The velocity of blood decreases for an increasing in the Hartmann number M , this decrease is caused by the interaction between magnetic field in an electrically conducting fluid such as blood, and this resulted to a force called Lorentz force which retards the motion of the fluid, as depicted in **Figure 7**.

vii. We also studied the increase in the level of stenosis with other treatment parameters. It is noticed in Figure 8 that the velocity decreases as stenosis increases. This result is of the view that the increase inhibits the regular flow of the fluid through the irregular channel.

viii. **Figure 9** depicts that the increases in treatment increased the velocity of the fluid; this increase is seen as the effectiveness of the treatment through drugs and other medical procedures in preventing the increase in the area of stenosis.

ix. The ration of retardation and relaxation was investigated and results shown in **Figure 10** and **Figure 11**. It is seen in **Figure 10** that the velocity of the fluid decreases for an increase in the relaxation and retardation ratio, while retardation increase caused the fluid velocity to increases as seen in **Figure 11**.

x. The fluid temperature increases for the increase in height of stenosis, this increase is of the view that the temperature increase leads to blood thinning, and that caused an enhanced flow as seen in **Figure 12**.

xi. Increase in oscillation caused a corresponding increase in temperature of the fluid as denoted using **Figure 13**. This result is of the view that as pulse frequency increases the temperature of the fluid also decreases.

xii. In investigating the effect of Schmidt number and radiation through a source on temperature, it is seen in **Figure 14** and **Figure 15**, in figure 14, the temperature increases for an increase in Schmidt number, while the temperature increases likewise for an increase in radiation parameter. This is consistent with existing laws of physics because increase in the radiation actually increases the temperature of the fluid which could lead to blood thinning.

xiii. The radiation absorption parameter increase led to an increase in fluid temperature, this of the view that there is an increase in retention level in the fluid and that caused the rise. But we noticed in **figure 17** that the temperature decreases for an increase in the treatment dosage.

xiv. The particles concentration was investigated in this research and results shown in **Figure 18**. This result shows that the particles concentration decreases for an increase in the chemical reaction between the palm oil and other constituents in the fluid. The concentration of the particles decreases as the Schmidt number is increased.

xv. The treatment parameters was investigated and found very effective because the fluid particle concentration increases for an increase in the treatment. This result clearly showed that the drug was able to block the production of more cholesterol into circulation.

In conclusion, we have able to model the problem under consideration, solved the analytically and simulated the results by varying the pertinent governing parameters to the satisfaction of the set out objectives.

ACKNOWLEDGMENT

The first Author would like to acknowledge and thank Tertiary Education Trust Fund (TETFUND) for funding his PhD programme, through which a lot of mathematical models were researched and developed to solve real-life problem.

REFERENCES

[1] Giua, L., Blasi, F., Simonetti, M. S., & Cossignani, L. (2013). Oxidative modifications of conjugated and unconjugated linoleic acid during heating. Food chemistry, 140(4) 680-685.

[2] Xian, T. K., Omar, N. A., & Ying, L. W. (2013). Reheated Palm Oil Consumption and Risk of Atherosclerosis: Evidence at Ultrastructural Level. Evid Based Complement Alterante Med 2012. Publication.

[3] Ng, C. Y., Leong, X. F., Masbah, N., Adam, S. K., Kamisah, Y., & Jaarin, K. (2014). Heated vegetable oils and cardiovascular disease risk factors. Vascular pharmacology, 61(1) 1-9.

[4] Baradaran, A., Nasri, H., & Rafieian-Kopaei, M. (2014). Oxidative stress and hypertension: Possibility of hypertension therapy with antioxidants.

Journal of research in medical sciences: the official journal of Isfahan University of Medical Sciences, 19(4) 358.
[5] Hausding, M., Jurk, K., Daub, S., Kröller-Schön, S., Stein, J., Schwenk, M., ... & Daiber, A. (2013). CD40L contributes to angiotensin II-induced pro-thrombotic state, vascular inflammation, oxidative stress and endothelial dysfunction. Basic research in cardiology, 108(6) 1-16.
[6] Swirski, F. K., & Nahrendorf, M. (2013). Leukocyte behavior in atherosclerosis, myocardial infarction, and heart failure. Science, 339(6116) 161-166.
[7] Kock, J. L. F., Pohl, C. H., & Venter, A. (2002). Super-oxidized soups and the health risks to poor South Africans: News an views. South African journal of science, 98(9) 413-414.
[8] Jaarin, K., Masbah, N., & Nordin, S. H. (2016). Heated cooking oils and its effect on blood pressure and possible mechanism: a review. Int J Clin Exp Med, 9(2) 626-636.
[9] Venkata, R. P., & Subramanyam, R. (2016). Evaluation of the deleterious health effects of consumption of repeatedly heated vegetable oil. Toxicology reports, 3, 636-643.
[10] Zhou, Z., Wang, Y., Jiang, Y., Diao, Y., Strappe, P., Prenzler, P., ... & Blanchard, C. (2016). Deep-fried oil consumption in rats impairs glycerolipid metabolism, gut histology and microbiota structure. Lipids in health and disease, 15(1) 1-11.
[11] Falade, A. O., Oboh, G., & Okoh, A. I. (2017). Potential health lmplications of the consumption of thermally-oxidized cooking oils–a review. Polish journal of food and nutrition sciences, 67(2).
[12] Kritchevsky, D., & Tepper, S. A. (1967). Cholesterol vehicle in experimental atherosclerosis: Part 9. Comparison of heated corn oil and heated olive oil. Journal of atherosclerosis research, 7(5) 647-651.
[13] Staprãns, I., Rapp, J. H., Pan, X. M., Hardman, D. A., & Feingold, K. R. (1996). Oxidized lipids in the diet accelerate the development of fatty streaks in cholesterol-fed rabbits. Arteriosclerosis, Thrombosis, and Vascular Biology, 16(4) 533-538.
[14] Staprans, I., Pan, X. M., Rapp, J. H., & Feingold, K. R. (1998). Oxidized cholesterol in the diet accelerates the development of aortic atherosclerosis in cholesterol-fed rabbits. Arteriosclerosis, thrombosis, and vascular biology, 18(6) 977-983.
[15] Odia, O. J., Ofori, S., & Maduka, O. (2015). Palm oil and the heart: a review. World journal of cardiology, 7(3) 144.
[16] Ong, A. S. H. (1994). Nutritional aspects of palm oil: an introductory review. Asia Pacific J Clin Nutr, 3, 201-206.
[17] Taghvaei, M., & Jafari, S. M. (2015). Application and stability of natural antioxidants in edible oils in order to substitute synthetic additives. Journal of food science and technology, 52(3) 1272-1282.
[18] Bunonyo, K. W., Israel-Cookey, C., & Amos, E. (2017). MHD Oscillatory Flow of Jeffrey Fluid in an Indented Artery with Heat Source. Asian Research Journal of Mathematics, 1-13.
[19] Bunonyo, K. W., & Amos, E. (2020). Lipid Concentration Effect on Blood Flow Through an Inclined Arterial Channel with Magnetic Field. Mathematical Modelling and Applications, 5(3) 129.
[20] Bunonyo, K. W., Amos, E., & Goldie, J. B. (2020). Mathematical Modelling of an Atherosclerotic Blood Flow Through Double Stenosed Region with Application of Treatment. International Journal of Applied Mathematics and Theoretical Physics, 6(2) 19.
[21] Bunonyo, K. W., & Eli, I. C. (2020). Mathematical Modeling of an Oscillatory MHD Blood Flow through a Lipid Saturated Porous Channel with Metabolic Heat and Magnetic Field. Communication in Physical Sciences, 6(1).
[22] Bunonyo, K. W., Amos, E., & Eli, I. C. (2018). Unsteady oscillatory couette flow between vertical parallel plates with constant radiative heat flux. Asian Research Journal of Mathematics, 1-11.

Nomenclature

x^*	Dimensional coordinate along the channel
y^*	Dimensional coordinate perpendicular to the channel
R	Radius of an abnormal channel
R_0	Radius of normal channel
R_T	Treatment parameter
d_0	Onset of stenosis
Rd_1	Heat radiation parameter
Rd_2	Radiation absorption parameter
Rd_3	Chemical reaction parameter
k_b	Thermal conductivity of blood
w^*	Dimensional velocity profile
w	Dimensionless velocity profile
w_0	Perturbed velocity profile
C	Concentration of lipoprotein-C

C_w Concentration at the wall

C_∞ Concentration at far field

c_{bp} The specific heat capacity of blood

t^* Dimensionless time

T Temperature of the fluid

T_∞^* Far field temperature

T_w^* Temperature at the wall

D_m Molecular diffusivity of lipoprotein-C concentration

B_0 Magnetic induction

Q_0 Dimensional thermal radiation

Q_1 Coefficient of proportionality for the radiation absorption

Greek Symbols

υ Kinematic viscosity of blood

μ_b Dynamic viscosity of blood

Pr Prandtl number for blood

g Acceleration due to gravity

δ^* Height of stenosis

σ_e Electrical conductivity

λ^* Length of stenosis

λ_1 The retardation time

λ_2 The ration of relaxation to retardation time

$\omega = 2\pi f_p$ Oscillatory frequency

ϕ Dimensionless Concentration

ϕ_0 Perturbed Concentration profile

θ Dimensionless Temperature

θ_0 Perturbed Temperature profile

ρ_b Density of the fluid

Subscripts

w Wall

b Blood

p Pulse